

Effect of Local Gear Tooth Failures on Gear Mesh Stiffness and Vibration Response of a Single-Stage Spur Gear Pair



M. Onkareshwar, Vamsi Inturi, S. P. Rajendra, P. K. Penumakala, and G. R. Sabareesh

Abstract Gears are positioned to transmit the power/torque and they are subjected to severe fluctuating speeds. The repetitive loading on the gear tooth may lead to failure which can cause plastic deformation and/or removal of contacting surfaces of tooth or even the initiation of fatigue crack. These tooth failures affect the transmission of gear and always accompanied by a variation in the gear mesh stiffness (GMS). In this work, both analytical and finite element (FE)-based numerical models are presented to estimate the GMS and also to extract the vibration response. A low-contact ratio, single-stage spur gear transmission consisting of eight degrees of freedom has been simulated. Two gear tooth failures, namely, tooth crack and breakage with two different severity levels are simulated. The effects of gear tooth failures on the evolution of GMS are compared with the case of ideal gear tooth. Further, frequency spectrum analysis is carried out to examine the effects of gear tooth failures on the amplitude of vibration of gear. Finally, the results of the developed analytical model and FE-based numerical model are validated with the experimental observations. It is observed that, the damaged gear tooth produces a reduction in the GMS values and lead to sidebands in the frequency spectrum.

Keywords Gear mesh stiffness · Tooth root crack · Tooth breakage · Vibration response

1 Introduction

Gearboxes act as a source of vibration because of the distinct load transmitted by the meshing of teeth. As they are expected to operate under severe fluctuating load/speeds, the repetitive loading takes place on the respective tooth of the gear pair which further could yield to the nucleation of crack at the fillet zone. Perhaps, failing in the early detection of this crack may result to initiate tooth chip and tooth

M. Onkareshwar · V. Inturi (✉) · S. P. Rajendra · P. K. Penumakala · G. R. Sabareesh
Department of Mechanical Engineering, BITS Pilani, Hyderabad 500078, India
e-mail: p20160025@hyderabad.bits-pilani.ac.in

© Springer Nature Singapore Pte Ltd. 2021

E. J. Sapountzakis et al. (eds.), *Proceedings of the 14th International Conference on Vibration Problems*, Lecture Notes in Mechanical Engineering, https://doi.org/10.1007/978-981-15-8049-9_69

1095

breakage which even may account for catastrophic failure [1]. In order to avoid these sudden failures and breakdowns, it is necessary to accomplish the health monitoring of the gearbox. The application of physical models is extensive in this field as they closely mimic with the object under study. The gear mesh stiffness (GMS) is instant based and it provides insight about the several gear properties such as load distribution, fatigue, vibration, etc. The GMS of the fault contained tooth is less compared with healthy gear tooth. Past researchers have examined the behaviour of GMS to quantify the severity of the gear tooth fault. Chaari et al. [2] proposed an analytical model to examine the effect of tooth breakage and spalling on the GMS of a single-stage spur gearbox. The authors have used potential energy method to calculate GMS and computed dynamic response for healthy and faulty cases of the gear tooth. Pandya and Parey [3] have studied the effect of different crack propagations and gear parameters (backup ratio, pressure angle and rim thickness) on GMS of a spur gear pair. Chen and Shao [4] have examined the effects of gear tooth crack nucleation along tooth depth and width on GMS of a spur gear transmission. Further, they have simulated the dynamic response using ODE45. Chen et al. [5] proposed an improved analytical model to estimate the GMS of a spur gear transmission having non-uniformly distributed fatigue crack over the width of the tooth. Finite element (FE) method offers competency in the simulation of GMS with different tooth profiles. Wang and Howard [6] have developed various FE models for the calculation of spur gear torsional mesh stiffness. Kiekbusch et al. [7] has developed two- and three-dimensional FE models to calculate the GMS. Pandya and Parey [8] have studied the crack behaviour and in a high contact ratio spur gear and its effect on GMS by FE method.

The majority of the existing literature focussed only on modelling the gearbox or analysing the response or model validation. This investigation aims to bridge all these analyses together. In this work, both analytical and FE-based numerical models are proposed to estimate the GMS of a low-contact ratio and single-stage spur gear transmission. Potential energy approach is used to estimate the GMS by considering the bending, fillet and contact deformations. Two gear tooth failures, namely, tooth root crack and breakage with two different severity levels are simulated. The effects of gear tooth failures on the evolution of GMS are compared with the case of an ideal gear tooth. Further, the vibration response of the system is simulated and the frequency spectrum is examined. Finally, the proposed analytical and FE-based numerical models are validated with the experimental observations.

2 Mathematical Modelling

2.1 Analytical Formulation of Gear Mesh Stiffness

GMS is time-varying parameter and is a function of the geometry of tooth, position of tooth contact, deflections of tooth and of course the defects present on the tooth.

Potential energy/lumped parameter approach is used in this study to achieve the GMS. In this approach, the gear tooth is treated as a non-uniform cantilever beam and the concepts of gear dynamics and beam theory are applied to calculate the GMS. The GMS of a single tooth is a combination of bending (δ_b), fillet foundation (δ_f) and contact (δ_h) defections. The deflection due to bending is calculated [9] by using the Eq. 1

$$\delta_b = F \cos^2 \alpha_m \sum_{i=1}^n e_i \left\{ \frac{(d_i^2 - e_i d_i + \frac{1}{3} e_i^2)}{\bar{E} \bar{I}_i} + \frac{1}{s_h G \bar{A}_i} + \frac{\tan^2 \alpha_m}{\bar{A}_i \bar{E}} \right\} \quad (1)$$

The corresponding bending stiffness (K_b) = F/ δ_b . The fillet foundation deflection is obtained [10] by using the Eq. 2

$$\delta_f = \frac{F \cos^2 \alpha_m}{WE} \left\{ L * \left(\frac{u_f}{S_f} \right)^2 + M * \left(\frac{u_f}{S_f} \right) + P * (1 + Q * \tan^2 \alpha_m) \right\} \quad (2)$$

The corresponding fillet-foundation stiffness (K_f) = F/ δ_f . The contact deflection is determined [11] by using the Eq. 3

$$\delta_h = \frac{\pi EW}{4(1 - \nu^2)} \quad (3)$$

The corresponding local contact stiffness (K_h) = F/ δ_h . For a single pair of gear teeth that are in meshing, the GMS (K_e) can be computed using Eq. 4

$$K_e = \frac{1}{\frac{1}{K_{b1}} + \frac{1}{K_{f1}} + \frac{1}{K_{b2}} + \frac{1}{K_{f2}} + \frac{1}{K_h}} \quad (4)$$

where ‘F’ is the applied force, ‘W’ is the tooth width, ‘ α_m ’ is pressure angle, ‘ ν ’ is the Poisson’s ratio, ‘ s_h ’ is a shear factor, ‘G’ is shear modulus and the details about the other terms (e_i , d_i , A_i , L , M , P , Q , u_f & s_f) are available in Chaari et al. [12].

A simple straight line crack is seeded at the root of the tooth and it is distributed along the width of the tooth [4]. The nucleation of crack at the root reduces the thickness of the tooth in the direction of tooth width (W) and this will become the new thickness value for computing the tooth deflections. Further, GMS is calculated with the help of Eq. 4 by considering the reduction in the tooth thickness. In this current study, two different severity levels of gear tooth root crack are approximated, one is up to half of the tooth thickness (50% RC) and the second one is up to 90% of the tooth thickness and attributed as 100% RC. On the other hand, tooth breakage arises because of the cyclic stressing/high-stress concentration of the gear tooth beyond its endurance strength, fatigue loading and overload [12]. The initiation of tooth breakage (say width W_b) reduces the available width (W) and this will be the new width of the tooth (W1) for calculating the tooth deflections. Further, GMS is computed according to the Eq. 4 by taking the reduction in the tooth width. In this

current study, two different severity levels of gear tooth breakage are seeded, one is up to half of the tooth width (50% TC) and the second one is up to 90% of the tooth width and attributed as 100% TC.

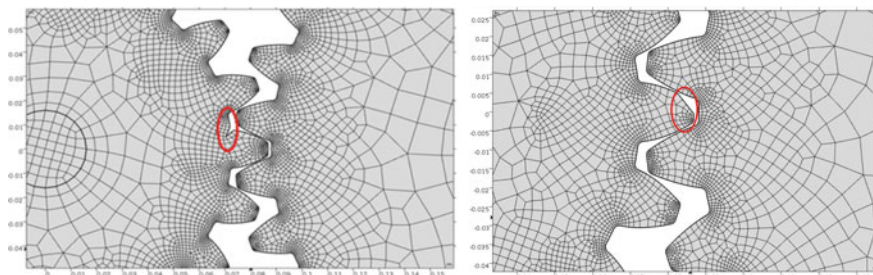
2.2 Finite Element Modelling

The finite element (FE) model of the spur gear has been generated using COMSOL Multiphysics v5.3. The model has been meshed using free quadrilateral elements with 17210 domain elements and 2746 boundary elements and number of degrees of freedom solved for: 37117 in the healthy case. Different geometric models have been created using the COMSOL part library for healthy, root crack and the tooth crack case with. To study the contact interaction between the gear pair, contact pairs were defined and the subsequent analysis was carried out. The pinion was given a prescribed angular displacement to have two meshing cycles. Hinge joints were provided for constraining the motion to one rotational degree of freedom. The following gear models have been analysed for the GMS, refer Fig. 1.

2.3 Dynamic Model of Single-Stage Spur Gear Pair

Dynamic models are developed on the basis of gear dynamics and tooth mesh mechanism to simulate the gearbox system response. Each gear/pinion is approximated as rigid plate having a hole at centre. In this study, lumped parameter modelling is performed to extract the vibration response from the single-stage spur gear pair. It is quite difficult to model all the details of the gearbox as such few hypotheses considered for modelling the gear pair. Those are as written below.

1. The gear material is homogeneous and the applied load is distributed uniformly along the width of the tooth,



(a) Pinion with tooth root crack

(b) Pinion with tooth breakage

Fig. 1 FE mesh of the spur gear pair models

Fig. 2 Single-stage spur gear pair model

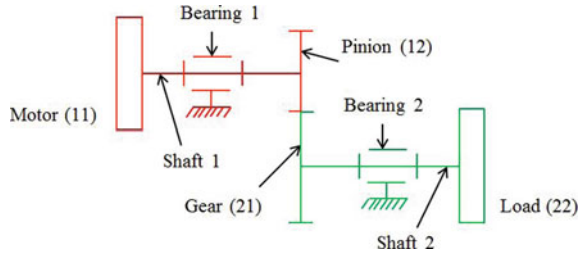


Table 1 Spur gear pair specifications

Parameter	Pinion (12)	Gear (21)
Number of teeth	20	80
Mass (kg)	0.6	6
Diameter of base circle (mm)	28.19	112.76
Contact ratio	1.6	1.6
Rotational speed (rpm)	187.5	46.875
Pressure angle (degrees)	20	20
Width of teeth (mm)	30	30
Gear mesh frequency (Hz)	62.5	
Motor inertia (kg m ²)	4.3*10 ⁻³	
Inertia of load (kg m ²)	1.25*10 ⁻³	
Bearing stiffness (N m ⁻¹)	1*10 ⁸	
Shaft torsional stiffness (N m ⁻¹)	1*10 ⁵	

2. The model ignores misalignment errors, transmission errors, friction between the gear teeth, backlash and environmental noise.

Figure 2 illustrates the schematic diagram of the dynamic model of a gear pair having eight degrees of freedom (DOFs). The pinion (12) is driven by a motor (T_m) and the gear (21) is loaded with inertia wheel (T_l). Shafts are braced on two bearings and each bearing is modelled by a linear spring. The GMS is time-varying because of the variation in the contact position of the teeth and variation in the number of teeth in mesh. The additional specifications about the spur gear pair are provided in Table 1. The vibration response of the system is obtained by the Eq. 5.

$$M\ddot{q} + K(t)q = F \tag{5}$$

where, ‘ M ’ is the mass matrix = diagonal ($m_1, m_1, I_{11}, I_{12}, m_2, m_2, I_{21}, I_{22}$), ‘ q ’ is the vector of DOFs = ($x_1, y_1, \theta_{11}, \theta_{12}, x_2, y_2, \theta_{21}, \theta_{22}$)^T, ‘ F ’ is the vector of applied forces = (0, 0, T_m , 0, 0, 0, 0, T_l)^T and ‘ $K(t)$ ’ is the global gear mesh stiffness matrix [2].

3 Results & Discussions

3.1 Comparison of Gear Mesh Stiffness

Since the contact ratio (1.6) is between 1 and 2, single tooth pair and double tooth pair contact take place during meshing of the tooth. In this study, it is approximated that the tooth engagement starts with double tooth pair contact and then single pair tooth contact occurs and finally tooth disengagement ends with double pair tooth contact [13]. This yields for the generation of time-varying GMS and this is the source of excitation of the gear pair. The time-varying GMS is calculated as explained in the Sect. 2 for the contact points of the gear pair and it is attributed as the total effective GMS. Figure 3 illustrates the GMS evolution for healthy and pinion faulty test cases. It can be noted that, the GMS is lower when there is a defect in the gear tooth when compared with healthy case and the mean value of fluctuation of GMS for healthy case is 3.58×10^8 N/m. Also, there is a significant reduction in the GMS values as the severity of tooth defect progresses. This can be attributed to the fact that, nucleation of defect (either root crack or tooth breakage) affects the geometry of the tooth, which further gives rise to the three deflections of the gear tooth. The mean value of GMS is found to be 3.25×10^8 N/m, 2.87×10^8 N/m, 3.1×10^8 N/m and 2.75×10^8 N/m for 50% RC, 100% RC, 50% TC and 100% TC, respectively. Instead of comparing the GMS values of faulty cases to the healthy condition, a cumulative percentage reduction index (CPRI) is determined for comparing the GMS values for successive

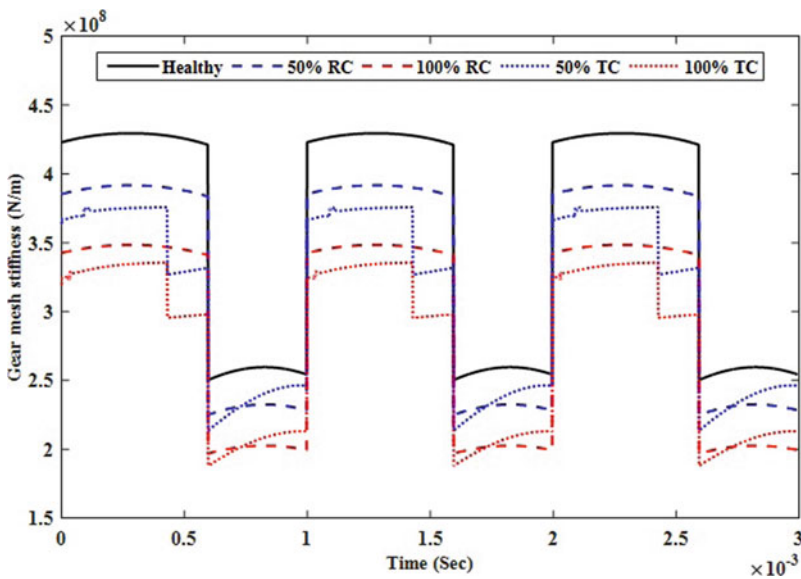


Fig. 3 Gear mesh stiffness evaluation for various test cases

severity levels [3].

$$CPRI = \left(\frac{K_i - K_{i-1}}{K_{i-1}} \right) * 100 \quad (6)$$

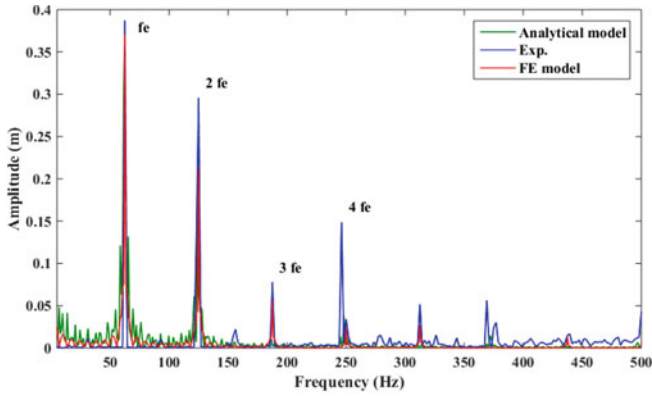
where K_i and K_{i-1} correspond to the reduction of GMS for two consecutive severity levels. The CPRI values for tooth root crack (RC) and tooth breakage (TC) are 13.06% and 12.92%, respectively.

3.2 Dynamic Response of the Gear Pair

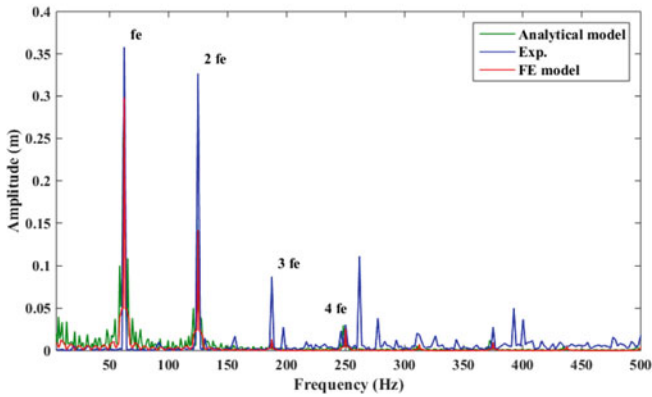
The computed GMS is utilized for simulating the vibration response of the spur gear transmission using ODE45 (Matlab subroutine) [4]. Figure 4 represents the frequency spectrum of the simulated vibration response (both analytical and FE model) as well as the experimentally measured vibration response. The frequency spectrum of the proposed analytical and FE models are validated with the frequency spectrum of the experimental data. It can be observed that, the healthy case spectrum contains the gear mesh frequency (f_e) and its harmonics. The component of ' f_e ' is quite dominant than the others ($2f_e$ and $4f_e$), refer Fig. 4a . The frequency spectrum of the proposed analytical model is validated with the frequency spectrum of the experimental data. In addition to the gear mesh frequency (f_e) and its harmonics ($2f_e$, $3f_e$ and $4f_e$) exist in the experimental frequency spectrum. However, nucleation of fault reduces the amplitude of the vibration response and this can be observed in the Fig. 4b and c. Alongside, the existence of fault yields for the sidebands (after 200 and 300 Hz) and these can be visible in the experimental frequency spectrum, refer Fig. 4b and c. It is worth noting that, the amplitude of vibration for experimental data is greater than the amplitude values of proposed analytical and FE models. This can be attributed to the fact that, there are interferences due to shafts and bearings in the actual case which may further result in the enhancement of the amplitude of vibration.

4 Conclusion

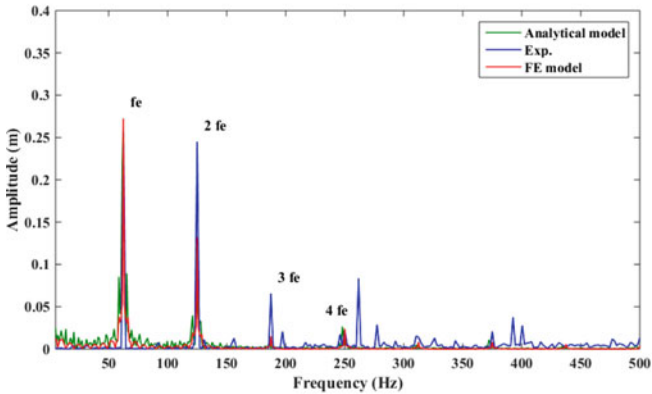
In this work, both analytical and FE-based numerical models are proposed to estimate the GMS of a single-stage spur gear pair. Potential energy approach is used to estimate the GMS by considering the bending, fillet and contact deformations. Two gear tooth failures, namely, tooth root crack and breakage with two different severity levels are simulated. The reduction in the gear mesh stiffness values is observed in the cases of tooth faults. Further, the dynamic response of the gear pair is computed and it shows the domination of gear mesh frequency (f_e) and its harmonics. Finally, the proposed physical models are validated with the experimental observations. The results obtained are in agreement with the literature.



(a) Healthy



(b) Gear tooth root crack (50% RC)



(c) Gear tooth breakage (50% TC)

Fig. 4 Frequency spectrum of vibration response of pinion

References

1. Vamsi I, Sabareesh GR, Penumakala PK (2019) Comparison of condition monitoring techniques in assessing fault severity for a wind turbine gearbox under non-stationary loading. *Mech Syst Sig Proc* 124:1–20
2. Chaari F, Baccar W, Abbes MS, Haddar M (2008) Effect of spalling or tooth breakage on gearmesh stiffness and dynamic response of a one-stage spur gear transmission. *Eur J Mech A Solids* 27(4):691–705
3. Pandya Y, Parey A (2013) Simulation of crack propagation in spur gear tooth for different gear parameter and its influence on mesh stiffness. *Eng Fail Anal* 30:124–137
4. Chen Z, Shao Y (2011) Dynamic simulation of spur gear with tooth root crack propagating along tooth width and crack depth. *Eng Fail Anal* 18(8):2149–2164
5. Chen Z, Zhai W, Shao Y, Wang K, Sun G (2016) Analytical model for mesh stiffness calculation of spur gear pair with non-uniformly distributed tooth root crack. *Eng Fail Anal* 66:502–514
6. Wang J, Howard I (2004) The torsional stiffness of involute spur gears. *Proc. Inst. Mech. Eng. [C] J Mech Eng Sci* 218(1):131–142
7. Kiekbusch T, Sappok D, Sauer B, Howard I (2011) Calculation of the combined torsional mesh stiffness of spur gears with two- and three-dimensional parametrical FE models. *Strojnicki Vestn-J Mech Eng* 57(11)
8. Pandya Y, Parey A (2013) Crack behavior in a high contact ratio spur gear tooth and its effect on mesh stiffness. *Eng Fail Anal* 34:69–78
9. Weber C (1949) The deformation of loaded gears and the effect on their load carrying capacity. Sponsored research (Germany), British department of science and industry research, p 3
10. Sainsot P, Vexel P, Duverger O (2004) Contribution of gear body to tooth deflections-a new bidimensional analytical formula. *Trans Am Soc Mech Eng J Mech Des* 126(4):748–752
11. Yang DCH, Sun ZS (1985) A rotary model for spur gear dynamics. *J Mech Transmissions Autom Des* 107:529
12. Chaari F, Fakhfakh T, Haddar M (2009) Analytical modelling of spur gear tooth crack and influence on gearmesh stiffness. *Eur J Mech A Solids* 28(3):461–468
13. Raghuvanshi NK, Parey A (2017) Experimental measurement of spur gear mesh stiffness using digital image correlation technique. *Measurement* 111:93–104